Journal of Organometallic Chemistry 694 (2009) 3134–3141

Contents lists available at ScienceDirect

Journal of Organometallic Chemistry

journal homepage: www.elsevier.com/locate/jorganchem

Formation and structural characterization of mercury complexes from $Te(R)CH_2SiMe_3$ (R = Ph, CH_2SiMe_3) and $HgCl_2$

Ludmila Vigo, Pekka Salin, Raija Oilunkaniemi *, Risto S. Laitinen *

Department of Chemistry, University of Oulu, P.O. Box 3000, FI-90014 Oulu, Finland

ARTICLE INFO

Article history:
Received 24 March 2009
Received in revised form 15 May 2009
Accepted 18 May 2009
Available online 23 May 2009

Keywords:
Telluroether
Mercury complex
X-ray crystallography
NMR spectroscopy

ABSTRACT

The reaction of $HgCl_2$ and $Te(R)CH_2SiMe_3$ [R = CH_2SiMe_3 (**1**), Ph (**2**)] in ethanol yielded a mononuclear complex $[HgCl_2\{Te(R)CH_2SiMe_3\}_2]$ (R = Ph, **3a;** R = CH_2SiMe_3, **3b**). The recrystallization of **3a** or **3b** from CH_2Cl_2 produced a dinuclear complex $[Hg_2Cl_2(\mu\text{-}Cl)_2\{Te(R)CH_2SiMe_3\}_2]$ (R = Ph, **4a**; R = CH_2SiMe_3, **4b**). When **3a** was dissolved in CH_2Cl_2, the solvent quickly removed, and the solid recrystallized from EtOH, a stable ionic $[HgCl\{Te(Ph)CH_2SiMe_3\}_3]Cl\cdot 2EtOH$ (**5a**·2EtOH) was obtained. Crystals of $[HgCl_2\{Te(CH_2SiMe)_2\}]\cdot 2HgCl_2\cdot CH_2Cl_2$ (**6b**·$2HgCl_2\cdot CH_2Cl_2$) were obtained from the CH_2Cl_2 solution of **3b** upon prolonged standing. The complex formation was monitored by ^{125}Te-, and ^{199}Hg NMR spectroscopy, and the crystal structures of the complexes were determined by single crystal X-ray crystallography.

1. Introduction

Whereas mercury(II) halides have been reported to form a number of 1:1 and 1:2 complexes with organic telluroethers, their structural information is rather sparse [1,2]. The structurally characterized formal 1:1 $[HgX_2(L)]$ complexes comprise $[HgI_2(TePh_2)]_2$ [3], $[HgBr_2\{Te(C_6H_4OEt)(C_6H_3[NMe_2]Me)\}_2]$ [4], $[HgBr_2\{Te(C_6H_4OMe)(C_2H_4[NC_4H_8])\}]$ [5], and $[HgBr_2\{Te(C_2H_4[NC_4H_8])_2\}]$ [5]. Crystal structures of the formal 1:2 $[HgX_2(L)_2]$ complexes have been determined for $[HgI_2(TePh)_2]$ [6] and $[HgX_2\{Te(Ph)[C_6H_3(Me)(NCC_6H_4(NO_2))]\}]$ (X = Cl, Br) [7]. The bidentate ditelluroether ligand contains two tellurium donor atoms forming a chelate with the Hg center, and the complex can therefore formally be considered as a 1:2 complex [8].

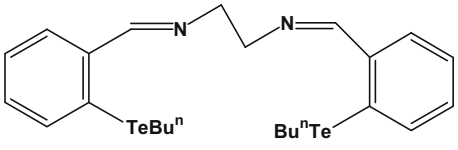

It has recently been reported that the palladium(II), platinum(II) [9–11], rhodium [12], and ruthenium(II) [13] complexes containing the $Te(CH_2SiMe_3)_2$ (**1**) [9] ligand show interesting stereochemical features. In this contribution we explored the ligand properties of **1** and related unsymmetric $Te(Ph)(CH_2SiMe_3)_2$ (**2**) towards the mercury(II) center. We report the formation of $[HgCl_2\{Te(R)CH_2SiMe_3\}_2]$ (R = Ph, **3a;** R = CH_2SiMe_3, **3b**), $[Hg_2Cl_2(\mu\text{-}Cl)_2\{Te(R)CH_2SiMe_3\}_2]$ (R = Ph, **4a;** R = CH_2SiMe_3, **4b**), $[HgCl\{Te(Ph)CH_2SiMe_3\}_3]Cl\cdot 2EtOH$ (**5a**·2EtOH) and $[HgCl_2\{Te(CH_2SiMe)_2\}]\cdot 2HgCl_2\cdot CH_2Cl_2$ (**6b**·$2HgCl_2\cdot CH_2Cl_2$). Small amounts of the last complex were formed upon prolonged standing of **3b** in CH_2Cl_2. The X-ray structures of **3a**, **4a**, **5a**·2EtOH, and **6b**·$2HgCl_2\cdot CH_2Cl_2$ are also described.

2. Experimental

2.1. General

All reactions and manipulations of air-sensitive reagents and those involving toxic mercury compounds were carried out under an argon atmosphere. $HgCl_2$ (Merck), Ph_2Te_2 (Aldrich), ethanol (Altia), dichloromethane (Lab-Scan), THF (Lab-Scan), and *n*-hexane (Lab-Scan) were used as purchased and without further purification. $PhTeCH_2SiMe_3$ was prepared according to the procedure described by Ogura et al. [14] and $Te(CH_2SiMe_3)_2$ was prepared by the method of Gysling et al. [9].

2.2. NMR Spectroscopy

$^{13}C\{^1H\}$, ^{125}Te, and ^{199}Hg NMR spectra were recorded on a Brucker DPX400 spectrometer operating at 100.61, 126.28, and 71.56 MHz, respectively. The respective spectral widths were 24.04, 126.58, and 100.00 kHz. The pulse widths were 11.00, 10.00, and 19.5 μs, respectively. $^{13}C\{^1H\}$ pulse delay was 2.00 s, that for ^{125}Te was 1.60 s, and for ^{199}Hg 0.1 s. $^{13}C\{^1H\}$, ^{125}Te, and

* Corresponding authors. Tel.: +358 8 553 1686 (R. Oilunkaniemi), tel.: +358 8 553 1611 (R.S. Laitinen).
E-mail addresses: raija.oilunkaniemi@oulu.fi (R. Oilunkaniemi), Risto.Laitinen@oulu.fi (R.S. Laitinen).

0022-328X/$ - see front matter © 2009 Elsevier B.V. All rights reserved.
doi:10.1016/j.jorganchem.2009.05.021

^{199}Hg accumulations contained ca. 1000, 30 000, and 10 000 transients, respectively. Tetramethylsilane was used as an external standard for ^{13}C chemical shifts. A saturated solution of Ph_2Te_2 in $CDCl_3$ and a 0.1 M solution of $HgCl_2$ in DMSO were used as external standards for ^{125}Te and ^{199}Hg chemical shifts, respectively. All spectra were recorded in THF. ^{13}C chemical shifts (ppm) are reported relative to Me_4Si, ^{125}Te chemical shifts are reported relative to neat Me_2Te [δ (Me_2Te) = δ (Ph_2Te_2) + 422] [15], and ^{199}Hg chemical shifts are reported relative to Me_2Hg [δ (Me_2Hg) = δ ($HgCl_2$ 1 M in DMSO-d6) − 1501] [16].

2.3. X-ray crystallography

Diffraction data of **3a**, **4a**, **5a**·2EtOH, and **6b**·$2HgCl_2{\cdot}CH_2Cl_2$ were collected on a Nonius Kappa-CCD diffractometer using graphite monochromated Mo Kα radiation (λ = 0.71073 Å; 55 kV, 25 mA). Crystal data and the details of structure determinations are given in Table 1.

Structures were solved by direct methods using SIR-92 [17] and refined using SHELXL-97 [18] After the full-matrix least-squares refinement of the non-hydrogen atoms with anisotropic thermal parameters, the hydrogen atoms were placed in calculated positions in the aromatic rings (C–H = 0.95 Å), in the CH_3 groups (C–H = 0.98 Å), and in the CH_2 groups (C–H = 0.99 Å). The scattering factors for the neutral atoms were those incorporated with the programs. WINGX user interface [19] was utilized throughout the structure solutions and refinements.

2.4. Preparation of the complexes

Two series of reactions were carried out by involving $HgCl_2$ and $Te(Ph)CH_2SiMe_3$ (**2**) or $Te(CH_2SiMe_3)_2$ (**1**) in molar ratios of 1:2, and 1:3. $HgCl_2$ was dissolved in 6 ml of ethanol and **2** or **1** were added into the solution that was subsequently stirred for 15 min at room temperature. The solvent was removed by evaporation. In case of the 1:2 reaction, $[HgCl_2\{Te(R)CH_2SiMe_3\}_2]$ (R = Ph **3a**, CH_2SiMe_3 **3b**) were formed. The 1:3 reaction also afforded **3a** or **3b** but in addition the reaction mixture contained unreacted ligand. The crude product was filtered and washed with cold ethanol. Upon recrystallization of the precipitate from CH_2Cl_2, dinuclear $[Hg_2Cl_2(\mu\text{-}Cl)_2\{Te(R)CH_2SiMe_3\}_2]$ (R = Ph **4a**, CH_2SiMe_3 **4b**) complexes were obtained. The yields of **4a** and **4b** could be optimized by involving the initial molar ratio of the reactants of 1:3. The amounts of starting materials, workup of the reaction solutions, optimized yields, elemental analyses, and NMR spectroscopic properties of the isolated products are listed below.

2.4.1. $[HgCl_2\{Te(R)CH_2SiMe_3\}_2]$ (R = Ph, **3a**; R = CH_2SiMe_3, **3b**)

Complex ***3a****:* $HgCl_2$ (0.101 g, 0.372 mmol), $Te(Ph)CH_2SiMe_3$ (0.225 g, 0.770 mmol). The crude product was recrystallized from ethanol, upon which a white crystalline solid of **3a** was formed. Yield 0.235 g (73.9%). Anal. Calc. for $HgCl_2Te_2C_{20}Si_2H_{32}$: C, 28.08; H, 3.77. Found: C, 27.68; H, 3.62%. $^{13}C\{^1H\}$ NMR: 137.0, 129.2, 127.2, 109.1 ppm (phenyl resonances), −1.1 ppm (CH_3), −9.9 ppm (CH_2); ^{125}Te NMR: 347 ppm (s), ^{199}Hg NMR: −1418 ppm (s).

Complex ***3b****:* $HgCl_2$ (0.100 g, 0.368 mmol), $Te(CH_2SiMe_3)_2$ (0.225 g, 0.745 mmol). The workup was carried out as for **3a**. White solid. Yield 0.241 g (74.7%). Anal. Calc. for $HgCl_2Te_2C_{16}Si_4H_{44}$: C, 21.94; H, 5.07. Found: C, 22.03; H, 4.89%. $^{13}C\{^1H\}$NMR: −1.1 ppm (CH_3), −7.4 ppm (CH_2); ^{125}Te NMR: 34 ppm (s), ^{199}Hg NMR: −1353 ppm (s).

2.4.2. $[Hg_2Cl_2(\mu\text{-}Cl)_2\{Te(R)CH_2SiMe_3\}_2]$ (R = Ph, **4a**; R = CH_2SiMe_3, **4b**)

Complex ***4a****:* $HgCl_2$ (0.105 g, 0.387 mmol), $Te(Ph)CH_2SiMe_3$ (0.338 g, 1.158 mmol). After evaporation of ethanol, 0.5 ml of

Table 1
Details of the structure determinations of $[HgCl_2\{Te(Ph)CH_2SiMe_3\}_2]$ (**3a**), $[Hg_2Cl_2(\mu\text{-}Cl)_2\{Te(Ph)CH_2SiMe_3\}_2]$ (**4a**), $[HgCl\{Te(Ph)CH_2SiMe_3\}_3]Cl{\cdot}2EtOH$ (**5a**·2EtOH), and $[HgCl_2\{Te(CH_2SiMe)_2\}]{\cdot}2HgCl_2{\cdot}CH_2Cl_2$ (**6b**·$2HgCl_2{\cdot}CH_2Cl_2$).

	3a	**4a**	**5a**·2EtOH	**6b**·$2HgCl_2{\cdot}CH_2Cl_2$
Empirical formula	$C_{20}H_{32}Cl_2HgSi_2Te_2$	$C_{20}H_{32}Cl_4Hg_2Si_2Te_2$	$C_{34}H_{60}Cl_2HgO_2Si_3Te_3$	$C_9H_{24}Cl_8Hg_3Si_2Te$
Relative molecular mass	855.33	1126.82	1239.38	1201.43
Crystal system	Monoclinic	Monoclinic	Triclinic	Triclinic
Space group	*C*2/*c*	$P2_1/n$	$P\bar{1}$	$P\bar{1}$
a (Å)	22.405(5)	6.2592(13)	13.371(3)	7.7139(15)
b (Å)	11.056(5)	16.072(3)	13.572(3)	12.763(3)
c (Å)	11.087(5)	15.017(3)	13.909(3)	15.710(3)
α (°)			71.19(3)	105.40(3)
β (°)	96.992(5)	94.94(3)	84.10(3)	100.27(3)
γ (°)			74.29(3)	106.05(3)
V (Å^3)	2725.9(18)	1505.1(5)	2299.6(8)	1379.2(5)
T (K)	120(2)	120(2)	120(2)	120(2)
Z	4	2	2	2
F(0 0 0)	1592	1024	1184	1068
D_c (g cm^{-3})	2.084	2.486	1.790	2.893
μ (Mo Kα) (mm^{-1})	8.033	12.531	5.432	18.550
Crystal size (mm)	0.30 × 0.15 × 0.10	0.20 × 0.10 × 0.08	0.20 × 0.20 × 0.09	0.30 × 0.20 × 0.09
θ Range (°)	1.83–26.00	3.50–25.99	2.55–26.00	1.76–26.00
Number of reflections collected	9966	22 897	33 473	17 702
Number of unique reflections	2686	2950	8907	5165
Number of observed reflections	2529	2768	7897	4350
Number of parameters	127	140	419	209
R_{int}	0.0757	0.1110	0.0880	0.1010
R_1[a,b]	0.0356	0.0374	0.0448	0.0557
wR_2[a,c]	0.0867	0.0849	0.1121	0.1505
R_1 (all data)[b]	0.0414	0.0428	0.0518	0.0675
wR_2 (all data)[c]	0.1065	0.0869	0.1179	0.1633
Goodness-of-fit (GOF)	1.212	1.122	1.050	1.059
Max. and min. heights in final difference Fourier synthesis (e Å^{-3})	2.766, −1.859	1.162, −1.562	1.050, −1.750	2.772, −1.852

[a] $I \geqslant 2\sigma(I)$.
[b] $R_1 = \sum||F_o| - |F_c||/\sum|F_o|$.
[c] $wR_2 = [\sum w(F_o^2 - F_c^2)^2/\sum wF_o^4]^{1/2}$.

CH_2Cl_2 was added and the solution was allowed to stay at room temperature for few minutes. The solvent was evaporated resulting in the formation of a yellow paste. 2 ml of *n*-hexane was added, the mixture was filtered, and the solution concentrated by evaporation of the solvent. Upon recrystallization of the crude product from CH_2Cl_2, a white crystalline solid of **4a** was obtained. Yield 0.135 g (70.7%). Anal. Calc. for $Hg_2Cl_4Te_2C_{20}Si_2H_{32}$: C, 21.32; H, 2.86. Found: C, 21.01; H, 2.64%. $^{13}C\{^1H\}$ NMR: 137.3, 129.6, 127.9, 113.7 ppm (phenyl resonances), −0.8 ppm (CH_3), −7. 1 ppm (CH_2); ^{125}Te NMR: 336 ppm (s), ^{199}Hg NMR: −1416 ppm (s).

Complex ***4b****:* $HgCl_2$ (0.102 g, 0.376 mmol), $Te(CH_2SiMe_3)_2$ (0.344 g, 1.139 mmol). The workup of the reaction solution was similar to that of **4a**. White solid. Yield 0.159 g (73.9%). Anal. Calc. for $Hg_2Cl_4Te_2C_{16}Si_4H_{44}$: C, 16.75; H, 3.87. Found: C, 16.92; H, 3.53%. $^{13}C\{^1H\}$ NMR: −0.4 ppm (CH_3), −1.0 ppm (CH_2); ^{125}Te NMR: 60 ppm (s), ^{199}Hg NMR: −1464 ppm (s).

2.4.3. [HgCl{Te(Ph)CH_2SiMe_3}$_3$]Cl·2EtOH (**5a**)

$HgCl_2$ (0.108 g, 0.398 mmol), $Te(Ph)CH_2SiMe_3$ (0.355 g, 1.216 mmol) When the crude product was dissolved in CH_2Cl_2, the solvent removed by evaporation after a few minutes, and the product was recrystallized from EtOH, white crystalline solid **5a** was obtained. Yield 0.370 g (75.1%). Anal. Calc. for $HgCl_2Te_3O_2C_{34}Si_3H_{60}$: C, 32.95; H, 4.88. Found: C, 32.61; H, 4.69%. $^{13}C\{^1H\}$ NMR: 137.1, 129.4, 128.1, 113.5 ppm (phenyl resonances), 57.4 ppm (ethanol CH_2), 18.5 ppm (ethanol, CH_3), −1.1 ppm (CH_3), −6.4 ppm (CH_2); ^{125}Te NMR: 304 ppm (s), ^{199}Hg NMR: −1055 ppm (s).

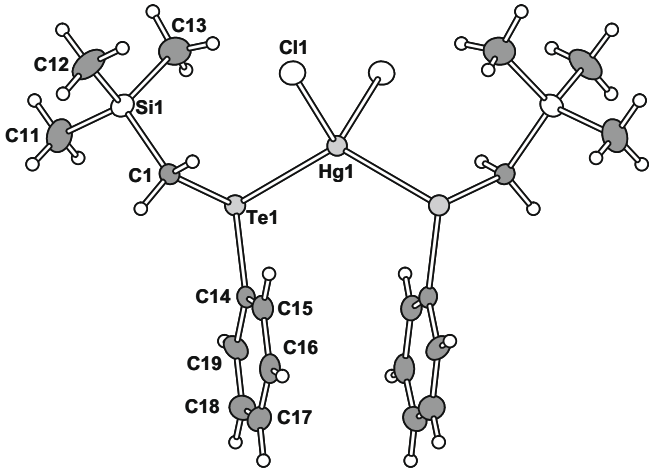

Fig. 1. The molecular structure of [$HgCl_2${Te(Ph)CH_2SiMe_3}$_2$] (**3a**) indicating the numbering of the atoms. Thermal ellipsoids are drawn at the 50% probability level.

2.4.4. [$HgCl_2${Te(CH_2SiMe)$_2$}]·2$HgCl_2$·CH_2Cl_2 (**6b**·2$HgCl_2$·CH_2Cl_2)

A small amount of crystals of [$HgCl_2${Te(CH_2SiMe_3)$_2$}]·2$HgCl_2$·CH_2Cl_2 (**6b**·2$HgCl_2$·CH_2Cl_2) were formed upon prolonged standing of [$HgCl_2${Te(CH_2SiMe_3)$_2$}$_2$] (**3b**) in ethanol. This product could only be characterized by single crystal X-ray crystallography.

3. Results and discussion

3.1. General

The reactions of one equivalent $HgCl_2$ with two equivalents of $Te(Ph)CH_2SiMe_3$ or $Te(CH_2SiMe_3)_2$ in ethanol affords good yields of [$HgCl_2${Te(R)CH_2SiMe_3}$_2$] (**3a** or **3b**). The reaction of one equivalent of $HgCl_2$ with three equivalents of $Te(Ph)CH_2SiMe_3$ or $Te(CH_2SiMe_3)_2$ in ethanol similarly yields **3a** and **3b**, but the reaction solution also contained unreacted ligand. Recrystallization of the crude product that were obtained from the above reactions by using CH_2Cl_2 affords dinuclear [Hg_2Cl_2(μ-Cl)$_2${Te(R)CH_2SiMe_3}$_2$] (R = Ph **4a** or CH_2SiMe_3 **4b**). **3a** and **3b** represent typical 1:2 complexes between $HgCl_2$ and the telluroether, and the latter pair (**4a** and **4b**) is formally a 1:1 complex that shows dinuclear association. If **3a** was dissolved in CH_2Cl_2, the solvent quickly removed, and the solid recrystallized from EtOH, a stable ionic [HgCl{Te(Ph)CH_2SiMe_3}$_3$]Cl·2EtOH (**5a**·2EtOH) was obtained. Upon prolonged standing of **3b** in CH_2Cl_2 for several weeks, a small amount of crystals of [$HgCl_2${Te(CH_2SiMe_3)$_2$}]·2$HgCl_2$·CH_2Cl_2 (**6b**·2$HgCl_2$·CH_2Cl_2) were obtained.

3.2. Crystal structures

3.2.1. [$HgCl_2${Te(Ph)CH_2SiMe_3}$_2$] (**3a**)

The crystal structure of **3a** is shown in Fig. 1 together with the atomic numbering scheme. Selected bond distances and bond angles are presented in Table 2. The structure consists of discrete complexes. The coordination sphere around the mercury atom is a distorted tetrahedron [the largest bond angle is Te(1)–Hg(1)–Te(1)[a] of 125.12(3)° and the smallest is Cl(1)–Hg(1)–Cl(1)[a] = 103.69(7)°] (for definition of the symmetry operation "a", see Table 2), typical of four-coordinated Hg(II) complexes [7,20–22]. The two symmetry-equivalent Hg–Te bonds show length of 2.7689(13) Å. It is consistent with the Hg–Te distance reported for [$HgCl_2${4-Ph(SB)Te}$_2$] (SB = 2-[4,4′-$NO_2C_6H_4CH$=NC_6H_3–Me]) (2.800(1)–2.773(1) Å) [7]. The two equivalent Hg–Cl bond lengths are 2.5202(15) Å. They are slightly longer than those in [$HgCl_2${4-Ph(SB)Te}$_2$] [2.496(2)–2.457(2) Å] [7].

The molecules are packed into two-dimensional planes (see Fig. 2). The complexes are linked together by Cl···H hydrogen bonds both in the plane and between the planes. The shortest in-plane hydrogen bond is 2.964(2) Å and that between the planes is

Table 2
Selected bond lengths (Å) and angles (°) of [$HgCl_2${Te(Ph)CH_2SiMe_3}$_2$] (**3a**), [Hg_2Cl_2(μ-Cl)$_2${Te(Ph)CH_2SiMe_3}$_2$] (**4a**), and [HgCl{Te(Ph)CH_2SiMe_3}$_3$]Cl·2EtOH (**5a**·2EtOH).

3a		4a		5a·2EtOH	
Hg(1)–Te(1)	2.7689(13)	Hg(1)–Te(1)	2.6796(7)	Hg(1)–Te(1)	2.7723(9)
Hg(1)–Cl(1)	2.5202(15)	Hg(1)–Cl(1)	2.6931(17)	Hg(1)–Te(2)	2.7771(8)
		Hg(1)–Cl(2)	2.3842(17)	Hg(1)–Te(3)	2.7497(10)
				Hg(1)–Cl(1)	2.5667(18)
Cl(1)–Hg(1)–Te(1)	105.59(4)	Cl(1)–Hg(1)–Te(1)	102.74(4)	Te(1)–Hg(1)–Te(2)	111.84(3)
Cl(1)–Hg(1)–Te(1)[a]	107.50(4)	Cl(2)–Hg(1)–Te(1)	144.66(4)	Te(1)–Hg(1)–Te(3)	114.14(3)
Te(1)–Hg(1)–Te(1)[a]	125.12(3)	Cl(1)–Te(1)–Cl(2)	103.52(6)	Te(2)–Hg(1)–Te(3)	113.53(2)
Cl(1)–Hg(1)–Cl(1)[a]	103.69(7)	Cl(1)–Hg(1)–Cl(1)[b]	86.98(5)	Te(1)–Hg(1)–Cl(1)	112.35(5)
		Hg(1)–Cl(1)–Hg(1)[b]	93.02(5)	Te(2)–Hg(1)–Cl(1)	101.81(5)
				Te(3)–Hg(1)–Cl(1)	102.09(5)

[a] Symmetry operations: $-x, y, -z+\frac{1}{2}$.
[b] Symmetry operations: $-x+1, -y, -z+2$.

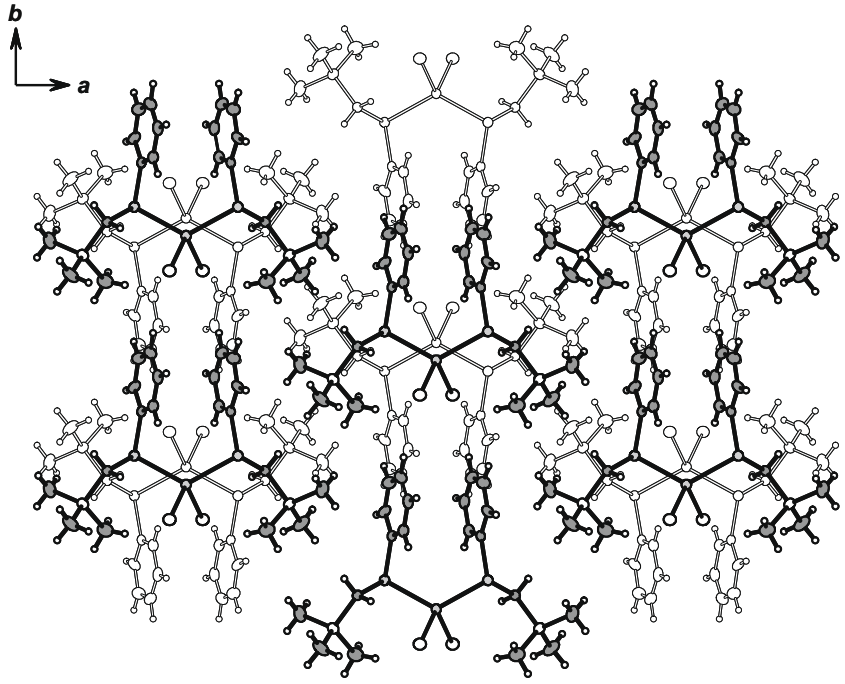

Fig. 2. The layer structure of **3a** in the solid lattice.

2.865(1) Å. In addition, there is an intramolecular H···Cl hydrogen bond of 2.915(2) Å between one of the methylene hydrogen atoms and chlorine.

3.2.2. $[Hg_2Cl_2(\mu\text{-}Cl)_2\{Te(Ph)CH_2SiMe_3\}_2]$ (**4a**)

The molecular structure of **4a** with the atomic numbering scheme is shown in Fig. 3 and the selected bond distances and angles are shown in Table 2. The formally 1:1 complex of $HgCl_2$ and $Te(Ph)CH_2SiMe_3$ is associated by symmetry into a dinuclear complex, in which two mercury atoms are bridged by two chlorido ligands and also coordinated to one terminal chlorido and one telluroether ligand. The mercury atom exhibits a distorted pseudo-tetrahedral geometry. The smallest angle is Cl(1)–Hg(1)–$Cl(1)^b$ = 86.98(5)° and the largest angle is Te(1)–Hg(1)–Cl(2) = 144.66(4)° (for definition of the symmetry operation "b", see Table 2). These values are similar to those in $[Hg_2Cl_2(\mu\text{-}Cl)_2(SePPh_3)_2]$ [7], in which the bond angles at mercury span a range 88.3(1)–136.3(2)°. The bridging Cl–Hg–Cl arrangement is symmetric with both Hg(1)–Cl(1) and $Hg(1)^b$–Cl(1) bonds exhibiting virtually the same length of 2.6931(17) Å. These bridging bonds are expectedly longer than the terminal bond Hg(1)–Cl(2) of 2.3842(17) Å in agreement with the bond lengths in $[Hg_2Cl_2(\mu\text{-}Cl)_2(SePPh_3)_2]$ (2.781(7) and 2.332(7) Å) [21]. The terminal Hg–Cl bond length in $HgCl_2\{Te(Ph)CH_2SiMe_3\}$ (**3a**) [2.5202(17) Å] is between those of the bridging and terminal Hg–Cl bonds in the dinuclear **4a**. The terminal bond length Hg(1)–Te(1) of 2.6796(17) Å is shorter than that in **3a** [2.7689(13) Å].

The H···Cl hydrogen bonding network link the discrete $[Hg_2Cl_2(\mu\text{-}Cl)_2\{Te(Ph)CH_2SiMe_3\}_2]$ (**4a**) complexes into skewed stacks (see Fig. 4). The shortest intermolecular hydrogen bonds are 2.822(2) and 3.044(2) Å. In addition, there is one H···Cl close contact of 2.932(2) Å.

3.2.3. $[HgCl\{Te(Ph)CH_2SiMe_3\}_3]Cl{\cdot}2EtOH$ (**5a**2EtOH)

The structure of **5a**·2EtOH with the atomic numbering scheme is shown in Fig. 5. Selected bond lengths and angles are presented in Table 2. The structure consists of a $[HgCl\{Te(Ph)CH_2SiMe_3\}_3]^+$ cation and a Cl^- anion. Hg(1) shows a slightly distorted tetrahedral coordination geometry in which the Cl–Hg–Te angles span the range of 101.81(5)–112.35(5)° and the Te–Hg–Te angles are 111.84(3)–114.14(3)°. The Hg–Te and Hg–Cl bond lengths [2.7497(10)–2.7771(8) and 2.5667(18) Å, respectively] are similar to those in **3a** (see Table 2).

The cation and anion show Te···Cl close contacts of 3.399(1)–3.416(1) Å (see Fig. 6). The ions are also linked by two H···Cl hydrogen bonds of 3.052(2) and 3.148(2) Å. There are also hydrogen bonds between the anion and the solvent molecules. The H···Cl distances in the Cl···H–O arrangement involving the two ethanol molecules are 2.282(2) and 2.384(2) Å.

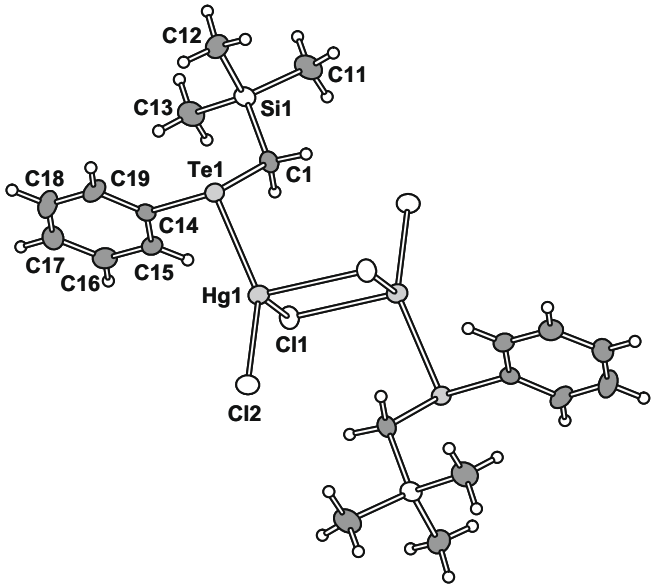

Fig. 3. The molecular structure of $[Hg_2Cl_2(\mu\text{-}Cl)_2\{Te(Ph)CH_2SiMe_3\}_2]$ (**4a**) indicating the numbering of the atoms. Thermal ellipsoids are drawn at the 50% probability level.

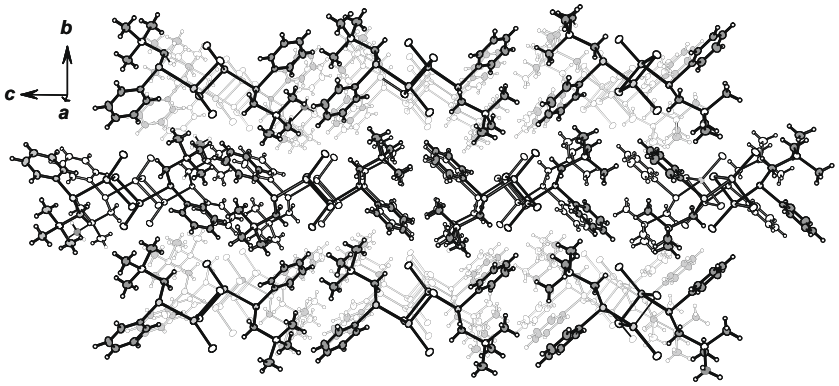

Fig. 4. The packing of discrete complexes **4a** into skewed stacks.

Only a few cationic mercury-chalcogen complexes are known in literature, as exemplified by $[CH_3HgSeC(NH_2)_2]NO_3$ [23] and $[HgCl(SeImMe)_3]Cl$ [SeImMe = tris(N-methyl-imidazoline-2-selenone)] [20]. The cation of the latter is analogous with that of **5a**.

3.2.4. $[HgCl_2\{Te(CH_2SiMe)_2\}]\cdot 2HgCl_2\cdot CH_2Cl_2$ (**6b**$\cdot 2HgCl_2\cdot CH_2Cl_2$)

The structure of **6b** with the atomic numbering scheme is shown in Fig. 7. Selected bond distances and bond angles are listed in Table 3. The lattice is formally composed of a 1:1 complex of $Te(CH_2SiMe_3)_2$ and $HgCl_2$, discrete $HgCl_2$ moieties, as well as the solvent of crystallization, CH_2Cl_2 (see Fig. 8). Mercury shows trigonal planar coordination ($\sum\alpha_{Hg} = 360°$), though the individual bond angles span a range 103.64(12)–139.83(10)°. The length of the Hg–Te bond is 2.6519(16) Å and those of the two Hg–Cl bonds are 2.429(4) and 2.542(3) Å. These values are quite consistent with those of other complexes considered in this paper. The Hg–Cl bond lengths in the two $HgCl_2$ units are 2.319(4)–2.346(3) Å (see Table 3). They deviate slightly from linearity [the two Cl–Hg–Cl bond angles are 171.06(12) and 172.45(13)°].

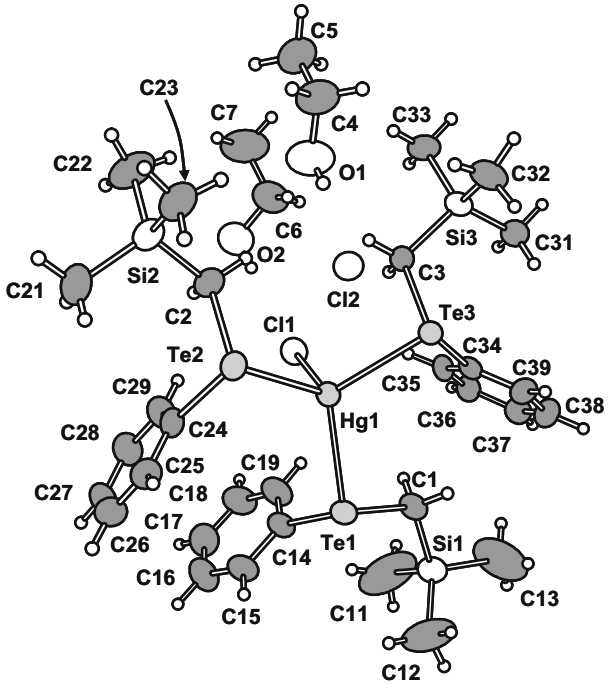

Fig. 5. The crystal structure of $[HgCl\{Te(Ph)CH_2SiMe_3\}_3]Cl\cdot 2EtOH$ (**5a**) indicating the numbering of the atoms. Thermal ellipsoids are drawn at the 50% probability level.

It can be seen from Fig 8a that the lattice consists of two-dimensional layers that are composed of alternating strands of $[HgCl_2\{Te(CH_2SiMe_3)_2\}]$ and $HgCl_2$. The **6b** complexes are linked into polymeric chains by two Hg···Cl interactions of 3.008(4) and 3.078(4) Å:

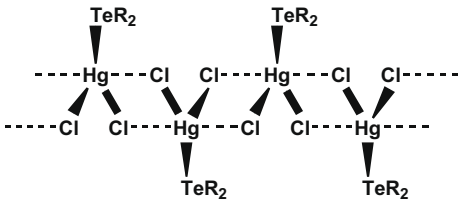

The Hg···Cl interactions expand the trigonal planar coordination of Hg(1) into a trigonal bipyramid (see Fig. 8). The two strands of $HgCl_2$ are also involved in Hg···Cl close contacts of 2.797(3)–3.329(4) Å. They expand the linear coordination of mercury atoms Hg(2) and Hg(3) into an octahedron. The H···Cl hydrogen bonds of 3.093(10) Å involving the dichloromethane solvent molecules link the layers into a three-dimensional structure (see Fig. 8b).

$[Hg_2Cl_2(\mu\text{-}Cl)_2(SEt_2)_2]\cdot HgCl_2$ shows a similar type of lattice with alternating stacks of dinuclear $[Hg_2Cl_2(\mu\text{-}Cl)_2(SEt_2)_2]$ complexes and $HgCl_2$ [24]. In a similar fashion as in **6b**$\cdot 2HgCl_2\cdot CH_2Cl_2$ the Hg···Cl contacts of 2.881–3.158 Å expand the coordination environment of the $HgCl_2$ mercury atom into an octahedron. Similarly, the distorted tetrahedron of the central atom in the dinuclear complex is expanded into an octahedron by two weak contacts of 3.558 Å.

3.3. NMR spectroscopy

3.3.1. Assignment of the resonances

All NMR spectra were recorded in THF. The ^{125}Te and ^{199}Hg chemical shifts are shown schematically in Fig. 9. It can be seen that both the ^{125}Te chemical shifts of **3a** (347 ppm) and **4a** (336 ppm) as well as their ^{199}Hg chemical shifts (−1416 and −1418 ppm, respectively) are virtually identical. Their ^{125}Te chemical shifts are also close to that of free $Te(Ph)CH_2SiMe_3$ (344 ppm in $CDCl_3$). The tellurium nucleus in **5a** is somewhat more shielded (304 ppm) than those of **3a** and **4a**. By contrast, the mercury nucleus of **5a** is less shielded (−1055 ppm) than those of **3a** and **4a**.

These two opposite trends can be explained by the relative electronegativities of the donor atoms to the central mercury. The distorted tetrahedral coordination environment of **3a** shows two tellurium and two chlorine donors, that of **4a** exhibits one tellurium and three chlorine donors two of which bridge two mercury centers, and that of **5a** coordinates to three tellurium and one chlorine donors. The shielding on tellurium decreases with increasing

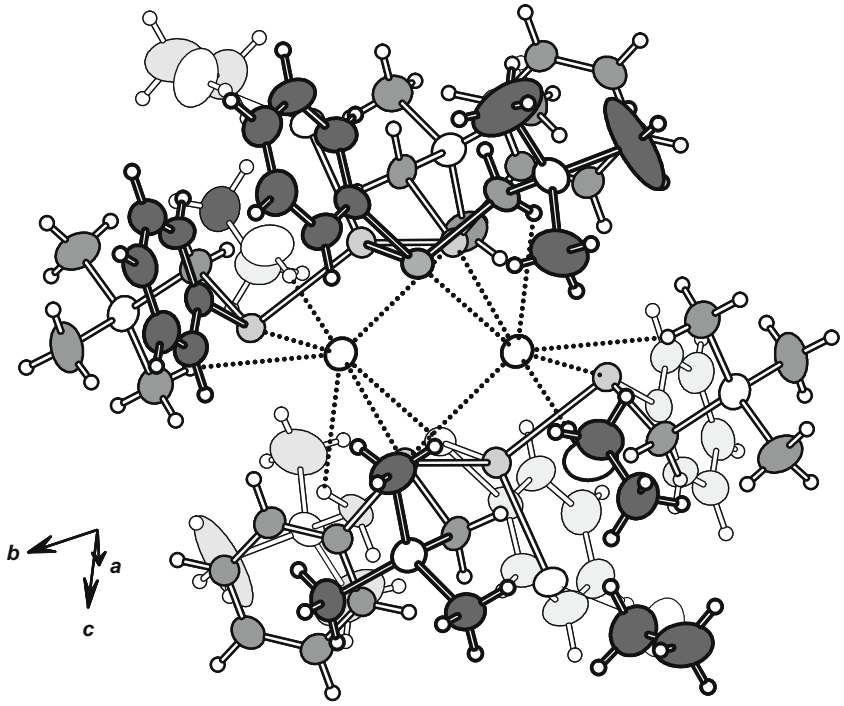

Fig. 6. Cation–anion interactions in **5a**·2EtOH.

number of more electronegative chlorido ligands that are coordinated to mercury. By contrast, the shielding of mercury increases with increasing number of chlorido ligands.

In the case of $Te(CH_2SiMe_3)_2$, the ^{125}Te chemical shifts of both **3b** and **4b** (36 and 60 ppm, respectively) lie at a slightly lower field to that of the free telluroether (26 ppm, see Ref. [10]). It is interesting to note that the ^{125}Te resonances of both **3b** and **4b** are found upfield from those of **3a** and **4a** (see Fig. 9). The smaller shielding of tellurium in case of **3a** and **4a** is probably caused by the presence of more electron withdrawing phenyl substituent on tellurium compared to that of Me_3SiCH_2-.

We further note that whereas the ^{199}Hg chemical shift of $[HgCl_2\{Te(CH_2SiMe_3)_2\}]$ (**3b**) lies upfield from that of $[HgCl_2\{Te(Ph)CH_2SiMe_3\}]$ (**3a**), that of $[Hg_2Cl_2(\mu\text{-}Cl)_2\{Te(CH_2SiMe_3)_2\}_2]$ (**4b**) lies downfield from $[Hg_2Cl_2(\mu\text{-}Cl)_2\{Te(Ph)CH_2SiMe_3\}_2]$ (**4a**). The presence of more electron withdrawing phenyl group again plays a role in this trend.

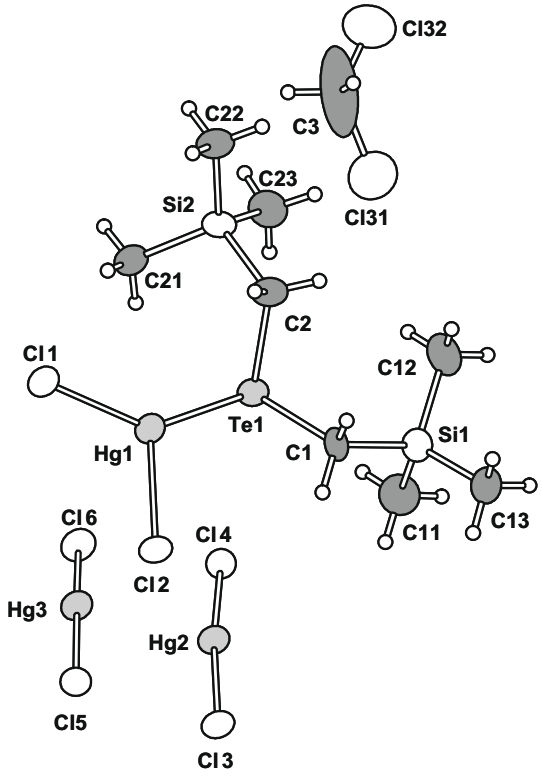

Fig. 7. The crystal structure of $[HgCl_2\{Te(CH_2SiMe)_2\}]\cdot 2HgCl_2\cdot CH_2Cl_2$ (**6b**·$2HgCl_2\cdot CH_2Cl_2$) indicating the numbering of the atoms. Thermal ellipsoids are drawn at the 50% probability level.

3.3.2. Interconversion pathways

All reactions were monitored by ^{125}Te NMR spectroscopy. The reaction solution from one equivalent of $HgCl_2$ and two equivalents of the ligands **2** or **1** in ethanol only showed one resonance due to **3a** or **3b**, respectively, as could be expected from a simple addition

Table 3
Selected bond lengths (Å) and angles (°) of $[HgCl_2\{Te(CH_2SiMe)_2\}]\cdot 2HgCl_2\cdot CH_2Cl_2$ (**6b**·$2HgCl_2\cdot CH_2Cl_2$).

Bond lengths	Å	Bond angles	°
Hg(1)–Te(1)	2.6519(16)	Te(1)–Hg(1)–Cl(1)	139.83(10)
Hg(1)–Cl(1)	2.429(4)	Te(1)–Hg(1)–Cl(2)	116.53(9)
Hg(1)–Cl(2)	2.542(3)	Cl(1)–Hg(1)–Cl(2)	103.64(12)
Hg(2)–Cl(2)	2.797(3)	Cl(2)–Hg(2)–Cl(3)	88.46(11)
Hg(2)–Cl(3)	2.346(3)	Cl(2)–Hg(2)–Cl(4)	91.48(11)
Hg(2)–Cl(4)	2.953(3)	Cl(2)–Hg(2)–Cl(5)	98.55(11)
Hg(2)–Cl(5)	2.342(3)	Cl(3)–Hg(2)–Cl(4)	94.12(11)
Hg(3)–Cl(4)	2.329(3)	Cl(3)–Hg(2)–Cl(5)	172.45(13)
Hg(3)–Cl(6)	2.319(4)	Cl(4)–Hg(2)–Cl(5)	88.52(11)
Hg(3)–Cl(1)[a]	2.985(3)	Cl(4)–Hg(3)–Cl(6)	171.06(12)
		Cl(4)–Hg(3)–Cl(1)[a]	102.72(11)
		Cl(6)–Hg(3)–Cl(1)[a]	86.16(12)
		Hg(1)–Cl(2)–Hg(2)	109.49(13)
		Hg(1)–Cl(1)–Hg(3)[a]	128.15(15)
		Hg(2)–Cl(4)–Hg(3)	94.09(12)

[a] Symmetry operation: $-x, -y, -z+1$.

reaction. In case of three equivalents of the ligand, the resonance of the unreacted ligand was also observed in addition to those of **3a** and **3b**.

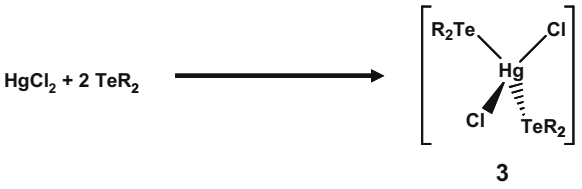

3

The solvent used for recrystallization plays a significant role in the formation of the end-products. The recrystallization of the crude product of the reaction of $HgCl_2$ and **2** or **1** from CH_2Cl_2 affords dinuclear complexes **4a** or **4b**, respectively. Their yields are maximized, when the molar ratio of $HgCl_2$ and the ligand is 1:3. This can be explained as follows: Upon short treatment of the crude product from the reaction of $HgCl_2$ and three equivalents of **2** with CH_2Cl_2 followed by recrystallization from EtOH, ionic $[HgCl\{Te(Ph)CH_2SiMe_3\}_3]Cl$ (**5a**) was obtained. Upon redissolving the crystals of **5a** in CH_2Cl_2, **4a** was again formed. This indicates that **5a** may be an intermediate in the formation of **4a** and rationalizes, why the yield of **4a** is maximized by using the molar ratio of 1:3 for $HgCl_2$ and **2**.

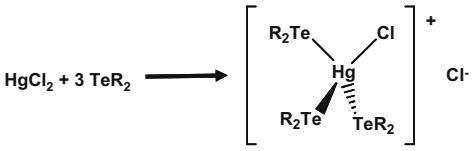

5

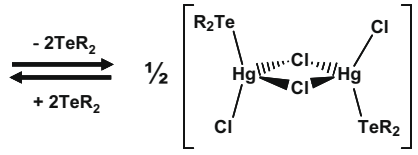

4

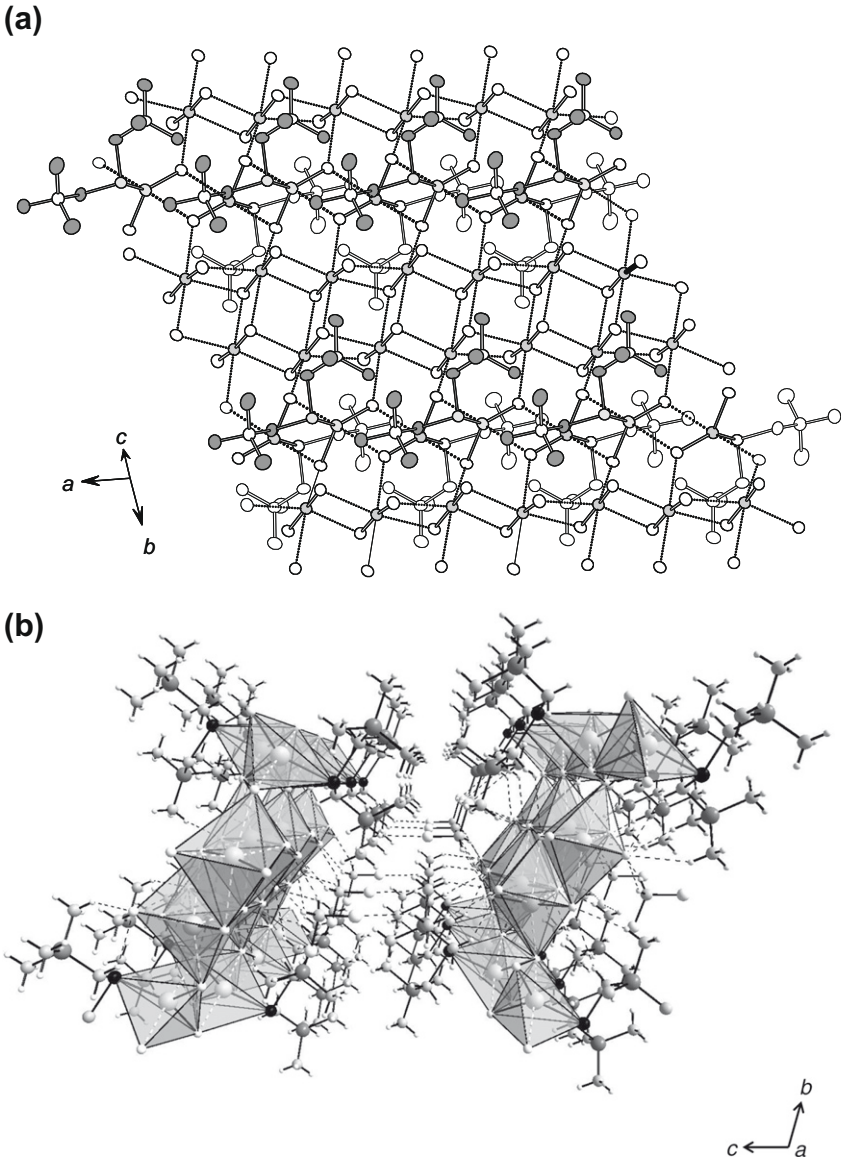

Fig. 8. The layer-like packing in $[HgCl_2\{Te(CH_2SiMe)_2\}]\cdot 2HgCl_2\cdot CH_2Cl_2$ (**6b**·$2HgCl_2\cdot CH_2Cl_2$). (a) The alternating strands of $[HgCl_2\{Te(CH_2SiMe_3)_2\}]_n$ and $HgCl_2$ are linked with Hg···Cl secondary bonding interactions expanding the coordination spheres of mercury into either an octahedron or a trigonal bipyramid. (b) H···Cl hydrogen bonds link the layers into a three-dimensional structure.

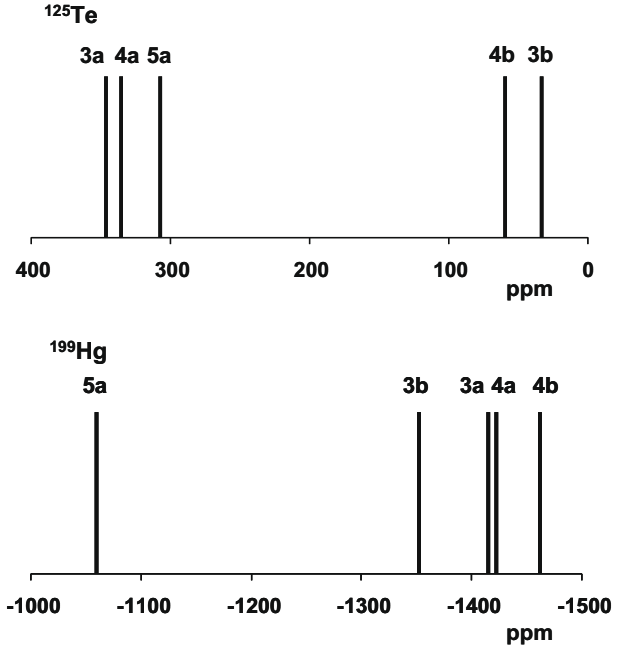

Fig. 9. The schematic overview of the ^{125}Te and ^{199}Hg chemical shifts of **3a**, **3b, 4a**, **4b**, and **5a**·2EtOH.

The formation of **6b** can be explained by the equilibrium between complexes **4** and **6** that show the same Hg:Cl:TeR_2 molar ratio.

We also note that when **3a** was dissolved in CH_2Cl_2, the ^{125}Te NMR resonances of dinuclear complexes $[Hg_2Cl_2(\mu\text{-}Cl)_2\{Te(Ph)CH_2SiMe_3\}_2]$ (**4a**) were observed in addition to that of the free ligand.

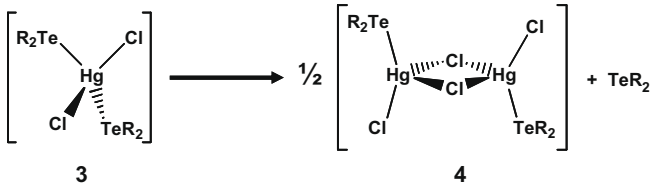

Furthermore, a resonance at 800 ppm was found in the spectrum. This resonance is tentatively assigned to $PhTeCl_2CH_2SiMe_3$ and could be due to the reaction of the excess ligand with Cl· radicals that are formed by the decomposition of CH_2Cl_2, since the reactions were carried out in light.

4. Conclusions

While the reactions of $HgCl_2$ with $Te(R)CH_2SiMe_3$ (R = Ph, CH_2SiMe_3) (molar ratio of 1:2) in ethanol affords a mononuclear complex $[HgCl_2\{Te(R)CH_2SiMe_3\}_2]$, the recrystallization from CH_2Cl_2 produces a dinuclear complex $[Hg_2Cl_2(\mu\text{-}Cl)_2\{Te(R)CH_2SiMe_3\}_2]$. The ionic complex $[HgCl\{Te(Ph)CH_2SiMe_3\}_3]Cl\cdot 2EtOH$ is isolated by treating $[HgCl_2\{Te(Ph)CH_2SiMe_3\}_2]$ with CH_2Cl_2 for a short time followed by recrystallization from EtOH. The products were characterized by X-ray crystallography as well as multinuclear NMR. The solid state lattices are formed by discrete molecular species or ions, but with extensive H···Cl hydrogen bonding network. In case of **6b**, significant secondary Hg···Cl bonding interactions are also observed.

Acknowledgments

Financial support from Academy of Finland and the Ministry of Education (L.V.) is gratefully acknowledged.

Appendix A. Supplementary material

CCDC 724692, 724693, 724694 and 724695 contain the supplementary crystallographic data for this paper. These data can be obtained free of charge from The Cambridge Crystallographic Data Centre via www.ccdc.cam.ac.uk/data_request/cif.

Supplementary data associated with this article can be found, in the online version, at doi:10.1016/j.jorganchem.2009.05.021.

References

[1] E.G. Hope, W. Levason, Coord. Chem. Rev. 112 (1993) 109.
[2] W. Levason, S.D. Orchard, G. Reid, Coord. Chem. Rev. 225 (2002) 159.
[3] F.W.B. Einstein, C.H.W. Jones, R.D. Sharma, Inorg. Chem. 22 (1983) 3924.
[4] B.L. Khandelwal, A.K. Singh, V. Srivastava, D.C. Povey, G.W. Smith, Polyhedron 9 (1990) 2041.
[5] G. Singh, A.K. Singh, P. Sharma, J.E. Drake, M.B. Hursthouse, M.E. Light, J. Organomet. Chem. 688 (2003) 20.
[6] E. Schulz Lang, C.C. Gatto, U. Abram, Z. Anorg. Allg. Chem. 628 (2002) 335.
[7] A.K.S. Chauhan, Anamika, A. Kumar, P. Singh, R.C. Srivastava, R.J. Butcher, J. Beckmann, A. Duthie, J. Organomet. Chem. 691 (2006) 1954.
[8] N. Al-Salim, T.A. Hamor, W.R. McWhinnie, J. Chem. Soc., Chem. Commun. (1986) 453.
[9] H.J. Gysling, H.R. Luss, D.L. Smith, Inorg. Chem. 10 (1979) 2696.
[10] L. Vigo, R. Oilunkaniemi, R.S. Laitinen, Eur. J. Inorg. Chem. (2008) 284.
[11] R. Oilunkaniemi, L. Vigo, M.J. Poropudas, R.S. Laitinen, Phosphorus, Sulfur, Silicon Relat. Elem. 183 (2008) 1046.
[12] L. Vigo, M.J. Poropudas, P. Salin, R. Oilunkaniemi, R.S. Laitinen, J. Organomet. Chem. 694 (2009) 2053.
[13] L. Vigo, M.J. Poropudas, R. Oilunkaniemi, R.S. Laitinen, J. Organomet. Chem. 693 (2008) 557.
[14] F. Ogura, T. Otsubo, N. Ohira, Synthesis (1983) 1006.
[15] H.C.E. McFarlane, W. McFarlane, J. Chem. Soc., Dalton Trans. (1973) 2416.
[16] M.A. Sens, N.K. Wilson, P.D. Ellis, J.D. Odom, J. Magn. Reson. 19 (1975) 323.
[17] A. Altomare, G. Cascarano, C. Giacovazzo, A. Gualardi, J. Appl. Crystallogr. 26 (1993) 343.
[18] G.M. Sheldrick, Acta Crystallogr. 64A (2008) 112.
[19] L.J. Farrugia, J. Appl. Cryst. 32 (1999) 837.
[20] A.D. Al-Amri, M. Fettouhi, M.I.M. Wazeer, A.A. Isab, Inorg. Chem. Commun. 8 (2005) 1109.
[21] L.S. Dent Glasser, L. Ingram, M.G. King, G.P. McQuillan, Inorg. Phys. Theor. (1969) 2501.
[22] N.A. Bell, T.N. Branston, W. Clegg, J.R. Creighton, L. Cucurull-Sanchez, M.R.J. Elsegood, E.S. Rapeer, Inorg. Chim. Acta 303 (2000) 220.
[23] A.J. Carty, S.F. Malone, N.J. Taylor, J. Organomet. Chem. 172 (1979) 201.
[24] C.-I. Braenden, Ark. Kemi 22 (1964) 83.